Ferrous tris(trimethylsilyl)silanolates: synthesis, structure, reactivity and thermal decomposition

A.N. Kornev [a,*], T.A. Chesnokova [a], V.V. Semenov [a], E.V. Zhezlova [a], L.N. Zakharov [a], L.G. Klapshina [a], G.A. Domrachev [a], V.S. Rusakov [b]

[a] *G.A. Razuvaev Institute of Organometallic Chemistry, Russian Academy of Sciences, Tropinin str., 49, 603600 Nizhny Novgorod, Russian Federation*

[b] *Department of Physics, Moscow State University, Moscow 119899, Russian Federation*

Received 5 December 1996

Abstract

Reaction of $FeBr_2$ with 3 equiv. of sodium tris(trimethylsilyl)silanolate (1) in DME affords the ate-complex $\{[(Me_3Si)_3SiOFe[\mu\text{-}OSi(SiMe_3)_3]_2Na(DME)\}$ (2). X-ray studies have shown the Fe atom in 2 is bonded to three O atoms of $OSi(SiMe_3)_3$ groups, two O atoms are connecting as a μ-bridge the $Fe[OSi(SiMe_3)_3]_3$ unit with the Na(DME) group. The FeO_3 core is slightly non-planar: the deviation of the Fe atom from the O_3 plane is 0.08 Å. The four-member $Fe(\mu\text{-}O)_2Na$ cycle is also non-planar: the dihedral angle between the $Fe(\mu\text{-}O)_2$ and the $(\mu\text{-}O)_2Na$ planes is 31.0°. The bridging and terminal Fe–O distances are 1.840(2) and 1.894(2), 1.910(2) Å, respectively. The average Si–Si and Si–C distances are 2.358(8) Å and 1.873(8) Å. Interaction of $FeBr_2$ with two equiv. of 1 in THF followed by treatment with pyridine yields the adduct, $[(Me_3Si)_3SiO]_2Fe(Py)_2$ (3). The Mössbauer spectrum of complex 2 at 295 K consists of a single doublet with isomer shift 0.60(1) mm/s and quadrupole splitting 0.90(3) mm/s. The corresponding parameters of 3 are as follows: isomer shift, 1.08(1) mm/s, and quadrupole splitting, 2.12(2) mm/s. Molecular oxygen is easily incorporated into the Si–Si bonds of compounds 2 and 3 by activation at the iron (II) center. Reaction of 2 with 1 equiv. of tetracyanoethylene leads to iron (III) silanolate. $[(Me_3Si)_3SiO]_3Fe$ (4) and the anion-radical salt. Na^+TCNE^-. Slow thermolysis of 2 and 3 yields $(Me_3Si)_3SiOSiMe_3$ and $(Me_3Si)_4Si$ as well as polyferrisiloxane with MW ~ 3500. Fast thermolysis results in formation of α-Fe and a complicated mixture of oligosiloxanes. © 1997 Elsevier Science S.A.

Keywords: Iron; Silanolates; X-ray diffraction; Mössbauer spectra

1. Introduction

Organotransition-metal complexes possessing a certain degree of unsaturation are of continuing interest both theoretically and experimentally [1]. In this regard the generation of compounds with novel ligands remains a critical problem. Compounds of two-valent three-coordinate iron are still quite rare. As to iron silanolates, there are no structurally characterised compounds until today. Here we wish to report the synthesis, Mössbauer spectra, reactivity towards oxidants and thermal decomposition of the first structurally characterised ferrous silanolate, $\{[(Me_3Si)_3SiO–Fe[\mu\text{-}OSiMe_3]_2Na(DME)\}$ together with the pyridine adduct. $(Me_3Si)_3SiO]_2Fe(Py)_2$.

2. Experimental

The solvents were purified prior to use following standard methods [2]. Tetracyanoethylene was purified by vacuum sublimation prior to use. All manipulations were performed in vacuo or under an argon atmosphere using standard Schlenk techniques.

2.1. Synthesis of $\{(Me_3Si)_3SiOFe[OSi(SiMe_3)_3]_2Na(DME)\}$ (2)

A solution of sodium tris(trimethylsilyl)silanolate (1) [3] (11.18 g, 39.0 mmol) in DME (50 ml) was added to a suspension of ferrous bromide (2.80 g, 13.0 mmol) in the same solvent (25 ml) at 20°C. Dissolution of $FeBr_2$ occurred immediately. The mixture was stirred for 2 h at 50°C. Dimethoxyethane was evaporated in vacuo and

---

replaced with 50 ml of hexane. Subsequent stirring 1 h and filtration of the NaBr precipitate yields a clear solution. Hexane was removed under reduced pressure. The crystalline solid was then filtered and recrystallised from warm hexane to provide 10.36 g (83%) of pale-green crystals. *Anal.* Calcd. for $C_{31}H_{91}O_5Si_{12}FeNa$: C, 38.79; H, 9.55; Fe, 5.82. Found: C, 38.10; H, 9.17; Fe, 5.52%. IR (cm^{-1}): 1240vs, 840vs, 675s, 620m (SiMe); 1070s(C–O, DME), 900m (FeOSi).

2.2. Synthesis of [(Me$_3$Si)$_3$SiO]$_2$Fe(Py)$_2$ (3)

A solution of sodium tris(trimethylsilyl)silanolate (1) (5.73 g, 20.0 mmol) in THF (30 ml) was added to a suspension of ferrous bromide (2.16 g, 10.0 mmol) in 20 ml THF. After heating for 1 h at 50°C THF was evaporated in vacuo and replaced with 30 ml of benzene. The white precipitate (NaBr) was removed by centrifugation and excess of pyridine (6.33 g, 80.0 mmol) was added. The greenish-gray solution rapidly turned rust-red. Filtration, concentration and crystallisation yielded red crystals of 3 (5.63 g, 76%). *Anal.* Calcd. for $C_{28}H_{64}Si_8O_2N_2$Fe: C, 45.36; H, 8.70; Fe, 7.53. Found: C, 44.95; H, 8.86; Fe, 7.61. IR (cm^{-1}): 1235vs, 830vs, 675s, 620s (SiMe); 1580m, 740m, 700m (Py); 910w (FeOSi). MW 755.2 (cryoscopy), calcd. 741.4.

2.3. Reaction of 2 with tetracyanoethylene

To a solution of 2 (2.88 g, 3.0 mmol) in DME (10 ml) was added a solution of 0.38 g (3.0 mmol) TCNE in 15 ml of DME. The mixture instantly turned dark-violet. Dimethoxyethane was removed under reduced pressure and replaced with hexane. A dark-violet precipitate of Na$^+$TCNE$^-$ is formed. Filtration followed by solvent evaporation in vacuo results in a rust-red waxy solid of iron(III) tris(trimethylsilyl) silanolate (4) (2.39 g, 94%). *Anal.* Calcd. for $C_{27}H_{81}Si_{12}O_3$Fe: C, 38.29; H, 9.64; Fe, 6.59. Found: C, 37.88; H, 9.83; Fe, 6.65. IR (cm^{-1}): 1240s, 840vs, 675s, 620m (SiMe), 940w (FeOSi).

2.4. Reaction of 2 with oxygen and subsequent hydrolysis

Dry oxygen (70 ml, 3.0 mmol) was slowly bubbled through a solution of 2 (2.88 g, 3.0 mmol) in 20 ml of benzene at 17°C. The pale-green solution turned pale-brown. Excess of water was added. The mixture was stirred for 20 min then filtered and concentrated. GLC analysis of the resulted solution on a 2 m column with 5% SE-30 at 100°C showed the presence of four compounds. Two of them were: (Me$_3$SiO)$_3$SiOH (the first, retention time 1 min 45 s) [4], (Me$_3$Si)$_3$SiOH (the last, retention time 4 min 45 s) [3]. The other two silanols, (Me$_3$SiO)$_2$(Me$_3$Si)SiOH (retention time 2 min 10 s) and Me$_3$SiO(Me$_3$Si)$_2$SiOH (retention time 2 min 50 s) were

separated by preparative GLC and characterised indirectly. After treatment each of them with a Me$_3$SiCl/Et$_3$N mixture they gave accordingly (Me$_3$SiO)$_3$SiSiMe$_3$, ^{1}H NMR (100 MHz, CDCl$_3$, 300 K) (δ, ppm): 0.03 (s, 9H, SiMe$_3$), 0.15 (s, 27H, OSiMe$_3$) and (Me$_3$Si)$_2$Si(OSiMe$_3$)$_2$, ^{1}H NMR (δ, ppm): 0.06 (s, 18H, SiMe$_3$), 0.10 (s, 18H, OSiMe$_3$) [5].

2.5. Measurements

Infrared spectra were recorded on a Perkin-Elmer 577 spectrometer from 4000 to 200 cm^{-1}.

^{57}Fe Mössbauer spectra were recorded at 298 K on a MS1101E spectrometer with a 10 mCi ^{57}Co/Rh source. The spectra were computer fitted using a SPECTR programme from MSTools programme complex [6] created at the Department of Physics of Moscow State University. The chemical isomer shift data were received relative to metallic iron.

Room-temperature magnetic moments were measured by the Faraday method.

The ESR spectra of the TCNE anion-radical were

Table 1
Summary of crystal and intensity collection data and refinement for 2

Empirical formula	$C_{31}H_{91}FeNaO_5Si_{12}$
Crystal system	Monoclinic
Space group	P2$_1$/n
Unit cell dimensions	$a = 14.131(5)$ Å
	$b = 21.134(4)$ Å
	$c = 20.291(5)$ Å
	$\beta = 90.40(2)°$
Volume	6059(3) Å^3
Z	4
Formula weight	960.0
Density (calc.)	1.052 mg/m^3
Absorption coefficient	0.522 mm^{-1}
Radiation	Mo Kα ($\lambda = 0.71073$ Å)
Temperature (K)	153
2θ Range	2.0
Scan type	2θ/θ
Index ranges	$-18 \leq h \leq 17$, $-6 \leq k \leq 27$,
	$-26 \leq l \leq 26$
Reflections collected	12125
Independent reflections	11582 ($R_{int} = 1.31\%$)
Observed reflections	7228 ($F > 4.0\sigma(F)$)
System used	Siemens SHELXTL plus
	(PC version)
Refinement method	Full-matrix least-squares
Quantity minimized	$\sum w(F_o - F_c)^2$
Weighting scheme	$w^{-1} = \sigma^2(F) + 0.0007F^2$
Number of parameters refined	815
Final R indices (obs. data)	$R = 3.67\%$, $wR = 4.12\%$
R indices (all data)	$R = 8.64\%$, $wR = 5.74\%$
Goodness-of-fit	1.21
Largest and mean Δ/σ	1.081, 0.031
Data-to-parameter ratio	8.9 : 1
Largest difference peak	0.37 e Å^{-3}
Largest difference hole	-0.29 e Å^{-3}

detected in DME solution on a ESR-200D SRC spectrometer.

Thermal decomposition was carried out in vacuo (or in an argon atmosphere) with a heating rate of 3° min^{-1}. The temperature range studied extended to 400°C.

Table 2
Atomic coordinates ($\times 10^5$) and equivalent isotropic displacement coefficients ($\text{Å}^2 \times 10^4$) in 2

	x	y	z	$U(\text{eq})$
Fe(1)	57266(2)	14622(2)	17887(2)	227(1)
Na(1)	42311(8)	22010(5)	24527(5)	363(3)
Si(1)	46523(5)	23789(3)	6940(3)	269(2)
Si(11)	30329(6)	25111(4)	4487(4)	375(3)
Si(12)	53216(6)	34023(4)	6949(4)	415(3)
Si(13)	52993(6)	17438(4)	−1454(3)	377(3)
Si(2)	44696(5)	6209(3)	28718(3)	277(2)
Si(21)	30482(6)	4583(4)	22769(4)	376(3)
Si(22)	40959(6)	8618(4)	39734(4)	421(3)
Si(23)	53058(6)	−3420(3)	28299(4)	354(2)
Si(3)	80873(5)	12133(3)	16607(3)	268(2)
Si(31)	88596(6)	22036(3)	16426(4)	408(3)
Si(32)	88441(6)	5685(4)	8816(4)	439(3)
Si(33)	84073(6)	7657(4)	27079(4)	370(3)
O(1)	48538(12)	20576(8)	14209(7)	318(6)
O(2)	50191(12)	12263(7)	25392(8)	277(5)
O(3)	69489(12)	12794(8)	15468(8)	309(6)
O(4)	32226(16)	29621(11)	29435(10)	621(8)
O(5)	51050(16)	28299(10)	31886(12)	657(9)
C(111)	29319(25)	30520(19)	−2846(17)	684(14)
C(112)	23995(23)	28969(15)	11457(17)	547(12)
C(113)	23906(25)	17598(17)	2358(17)	631(13)
C(121)	63823(34)	33494(22)	12446(31)	1249(25)
C(122)	45341(27)	40282(16)	10523(21)	739(16)
C(123)	56874(42)	36591(22)	−1428(23)	1225(25)
C(131)	66155(24)	17614(17)	−1381(14)	572(12)
C(132)	49320(30)	9023(15)	12(17)	679(14)
C(133)	48749(25)	19856(16)	−9859(14)	554(12)
C(211)	21251(23)	7(17)	27382(17)	597(13)
C(212)	25619(22)	12659(16)	20931(16)	527(11)
C(213)	32295(24)	595(16)	14633(16)	554(12)
C(221)	51779(26)	11436(19)	44211(15)	647(14)
C(222)	32079(27)	15188(19)	40157(16)	679(14)
C(223)	36009(30)	1507(20)	44037(17)	780(16)
C(231)	61481(22)	−4721(13)	35358(15)	469(10)
C(232)	59316(23)	−3850(14)	20231(15)	479(11)
C(233)	44228(25)	−10013(14)	28685(20)	645(14)
C(311)	83879(23)	27150(14)	23186(16)	501(11)
C(312)	87313(31)	26288(16)	8401(18)	753(16)
C(313)	101704(24)	21045(17)	17879(24)	806(17)
C(321)	100393(25)	3375(17)	12301(19)	675(14)
C(322)	90885(31)	9907(20)	857(18)	832(17)
C(323)	81595(28)	−1622(19)	7011(20)	807(16)
C(331)	74347(23)	10443(14)	32593(13)	473(11)
C(332)	84401(24)	−1207(15)	26972(16)	555(12)
C(333)	95640(27)	10152(18)	30842(19)	736(15)
C(1)	22371(27)	29154(20)	30292(18)	785(16)
C(2)	36631(32)	33449(18)	34159(19)	775(16)
C(3)	46691(32)	34074(18)	33146(21)	793(17)
C(4)	60802(31)	28213(23)	32747(25)	1029(21)

Equivalent isotropic U defined as one third of the trace of the orthogonalised U_{ij} tensor.

Table 3
Selected bond lengths (Å) and bond angles (°) in 2

Fe(1)–Na(1)	2.960(1)	Fe(1)–O(1)	1.910(2)
Fe(1)–O(2)	1.894(2)	Fe(1)–O(3)	1.840(2)
Na(1)–O(1)	2.297(2)	Na(1)–O(2)	2.348(2)
Na(1)–O(4)	2.373(3)	Na(1)–O(5)	2.344(3)
Si(1)–Si(11)	2.355(1)	Si(1)–Si(12)	2.361(1)
Si(1)–Si(13)	2.358(1)	Si(1)–O(1)	1.647(2)
Si(11)–C(111)	1.881(4)	Si(11)–C(112)	1.866(3)
Si(11)–C(113)	1.878(4)	Si(12)–C(121)	1.865(5)
Si(12)–C(122)	1.877(4)	Si(12)–C(123)	1.861(5)
Si(13)–C(131)	1.860(3)	Si(13)–C(132)	1.877(3)
Si(13)–C(133)	1.875(3)	Si(2)–Si(21)	2.361(1)
Si(2)–Si(22)	2.356(1)	Si(2)–Si(23)	2.355(1)
Si(2)–O(2)	1.644(2)	Si(21)–C(211)	1.879(4)
Si(21)–C(212)	1.876(3)	Si(21)–C(213)	1.875(3)
Si(22)–C(221)	1.870(4)	Si(22)–C(222)	1.874(4)
Si(22)–C(223)	1.876(4)	Si(23)–C(231)	1.876(3)
Si(23)–C(232)	1.868(3)	Si(23)–C(233)	1.872(3)
Si(3)–Si(31)	2.359(1)	Si(3)–Si(32)	2.350(1)
Si(3)–Si(33)	2.367(1)	Si(3)–O(3)	1.630(2)
Si(31)–C(311)	1.874(3)	Si(31)–C(312)	1.869(4)
Si(31)–C(313)	1.885(4)	Si(32)–C(321)	1.891(4)
Si(32)–C(322)	1.879(4)	Si(32)–C(323)	1.857(4)
Si(33)–C(331)	1.873(3)	Si(33)–C(332)	1.874(3)
Si(33)–C(333)	1.875(4)	O(4)–C(1)	1.408(5)
C(4)–C(2)	1.397(5)	O(5)–C(3)	1.392(5)
O(5)–C(4)	1.388(5)	C(2)–C(3)	1.444(6)
O(1)–Fe(1)–O(2)	98.3(1)	O(1)–Fe(1)–O(3)	129.7(1)
O(2)–Fe(1)–O(3)	131.4(1)	O(1)–Na(1)–O(2)	76.6(1)
O(1)–Na(1)–O(4)	135.0(1)	O(2)–Na(1)–O(4)	148.2(1)
O(1)–Na(1)–O(5)	116.9(1)	O(2)–Na(1)–O(5)	101.7(1)
O(4)–Na(1)–O(5)	70.3(1)	Si(11)–Si(1)–Si(12)	106.3(1)
Si(11)–Si(1)–Si(13)	107.2(1)	Si(12)–Si(1)–Si(13)	111.4(1)
Si(11)–Si(1)–O(1)	113.6(1)	Si(12)–Si(1)–O(1)	108.1(1)
Si(13)–Si(1)–O(1)	110.3(1)	Si(21)–Si(2)–Si(22)	108.7(1)
Si(21)–Si(2)–Si(23)	106.3(1)	Si(22)–Si(2)–Si(23)	109.7(1)
Si(21)–Si(2)–O(2)	107.8(1)	Si(22)–Si(2)–O(2)	109.3(1)
Si(23)–Si(2)–O(2)	114.8(1)	Si(31)–Si(3)–Si(32)	106.9(1)
Si(31)–Si(3)–Si(33)	106.4(1)	Si(32)–Si(3)–Si(33)	106.7(1)
Si(31)–Si(3)–O(3)	112.2(1)	Si(32)–Si(3)–O(3)	114.1(1)
Si(33)–Si(3)–O(3)	110.1(1)	Fe(1)–O(1)–Si(1)	88.9(1)
Fe(1)–O(1)–Na(1)	136.8(1)	Na(1)–O(1)–Si(1)	134.2(1)
Fe(1)–O(2)–Na(1)	87.8(1)	Fe(1)–O(2)–Si(2)	142.0(1)
Na(1)–O(2)–Si(2)	119.2(1)	Fe(1)–O(3)–Si(3)	155.2(1)

The products of thermal decomposition of 2 was studied using the GPC method. Gel permeation chromatography was performed using a Waters 410 instrument with UV and refractive index detection. The solvent used was THF and the porosites of the styrogel column used were 25 and 8 nm (elution rate 0.9 ml min^{-1}). The molecular weight distribution was determined using polystyrene and polypropylene standards.

Gas chromatography analyses of products of hydrolysis were carried out on a Tsvet-500 chromatograph, equipped with stainless steel columns 0.4 cm × 200 cm, packed with 5% SE-30 on Chromatone N-Super, with a thermoconductivity detector and with helium as carrier gas.
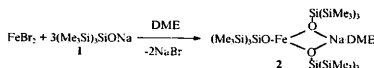
2.6. X-ray diffraction studies

Pale green crystals of **2** were grown by slow cooling to room temperature of a solution of the compound in hot hexane. The crystals were removed from a Schlenk tube under a stream of Ar and immediately covered with a layer of hydrocarbon oil. A suitable crystal was selected, attached with grease to a glass fiber and immediately placed in the low-temperature device of the X-ray diffractometer. All X-ray data were collected on a Siemens P3/PC diffractometer at 153 K. The structure of **2** was solved by direct methods. All non-H atoms were refined anisotropically. The H atoms were located in difference Fourier maps and refined isotropically. The final refinements converged at $R = 0.037$, $R_w = 0.041$, $S = 1.21$ for the observed reflections. The weight scheme was $w = 1/[\sigma^2(F) + 0.0007F^2]$. The $(\Delta/\sigma)_{av}$ value in the final cycles was 0.031. All calculations were performed using the SHELXTL-Plus programme [7]. The crystal data and some details of the data collection and refinement for **2** are given in Table 1. Atomic coordinates of non-hydrogen atoms and selected bond distances and angles for **2** are given in Tables 2 and 3, respectively. Full structural report for **2** including atomic coordinates bond lengths and angles, thermal parameters for all atoms is given in supplementary material.

3. Results and discussion

3.1. Synthesis and molecular structure

Reaction of 3 equiv. of sodium tris(trimethylsilyl) silanolate (**1**) with FeBr$_2$ in DME and subsequent re-

placement of DME with hexane results in formation of pale-green crystals of **2**.

$$FeBr_2 + 3(Me_3Si)_3SiONa \xrightarrow[-2NaBr]{DME} (Me_3Si)_3SiO-Fe \underset{O}{\overset{O}{<}} \begin{array}{c} Si(SiMe_3)_3 \\ \end{array} Na\cdot DME$$

X-ray study confirmed that the compound **2** is an ate-complex in which the Fe atom is bonded to three O-atoms of OSi(SiMe$_3$)$_3$ groups, two O atoms are connecting as a μ-bridge the Fe[OSi(SiMe$_3$)$_3$]$_3$ unit with the Na(DME) group (Fig. 1). The FeO$_3$ core of **2** is slightly non-planar: the deviation of the Fe(1) atom from the O$_3$ plane is 0.08 Å. The O(1)Fe(1)O(3) and O(2)Fe(1)O(3) angles (129.7(1) and 131.4(1)° are significantly larger than O(1)Fe(1)O(2) 98.3(1)° (Table 3). The FeOSi angles are in a wide range: Fe(1)–O(1)–Si(1) 136.8(1)°, Fe(1)–O(2)–Si(2) 142.0(1)°, Fe(1)–O(3)–Si(3) 155.2(1)°. The terminal Fe(1)–O(3) distance, 1.840(2) Å, is slightly shorter than the bridging Fe(1)–O(1) and Fe(1)–O(2) ones, 1.910(2) and 1.894(2) Å. The Si(3)–O(3) distance in the terminal OSi(SiMe$_3$)$_3$ group, 1.630(2), is also shorter than the lengths of similar bonds in the bridging ones Si(1)–O(1) 1.647(2) and Si(2)–O(2) 1.644(2) Å.

There are only a few X-ray structurally characterised low-coordinate Fe(II) complexes. The Fe–O(t) and Fe–O(b) distances found in **2** are very similar to those observed in two of them having a dimeric structure: 1.821(5), 2.027(5) Å in {Fe(OBMes$_2$)(μ-OBMes$_2$)}$_2$ [8] and 1.822(6), 2.016(6) Å in [Fe(O-2,4,6-t-Bu$_3$C$_3$H$_2$)$_2$]$_2$ [9], respectively. However, the differences between terminal and bridging distances in **2** (~ 0.07 Å) are less

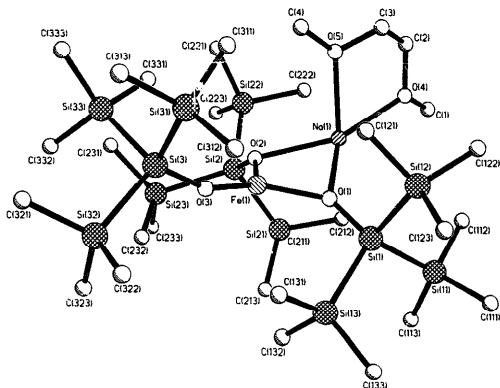Fig. 1. X-ray structure of **2** and atom labeling. The H atoms are omitted for clarity.

than those in the above mentioned aryl- and boryloxides (~ 0.18 Å).

The four-member $Fe(\mu\text{-O})_2Na$ cycle in 2 is non-planar: the dihedral angle between the FeO(1)O(2) and O(1)O(2)Na(1) planes is 31.0°. The distances between the Na atom and the μ-bridging O atoms (Na(1)–O(1) 2.297(2) and Na(1)–O(2) 2.348(2) Å are slightly shorter than the Na–O(DME) bond lengths (Na(1)–O(4) 2.374(3) and Na(1)–O(5) 2.344(3) Å).

The Si atoms in 2 have a distorted tetrahedral environment. The Si–Si and Si–C distances (2.350(1)–2.367(1) (average 2.358(8) Å) and 1.857(4)–1.891(4) Å (average 1.873(8) Å, respectively) are in the typical ranges for lengths of these bonds.

Interaction of $FeBr_2$ with 2 equiv. of 1 in THF followed by treatment with pyridine yields red crystals of adduct 3:

$$FeBr_2 + 2(1) \xrightarrow[\substack{2\text{)Py/PhH}}]{\substack{1\text{)THF, 20°C}}} \underset{3}{[(Me_3Si)_3SiO]_2Fe(Py)_2}$$

Although a quite pure sample of 3 was obtained, we have not yet been able to isolate crystals of this product suitable for X-ray study. Molecular weight measured by cryoscopy in benzene was found to be 755.2, that corresponds to monomeric 3 in solution.

3.2. Reactions

Compounds 2 and 3 are extremely oxygen and moisture sensitive. Hydrolysis of 2 in benzene solution is completed in a matter of seconds but 3 reacts for several minutes to give tris(trimethylsilyl)silanol and ferrous hydroxide. Interestingly, silanolates 2 and 3 are pyrophoric in the finely divided state. In benzene solution they are easily oxidised by oxygen. Subsequent hydrolysis of fully oxidised compounds yields tris(trimethylsiloxy)silanol, $(Me_3SiO)_3SiOH$. In the case of oxygen deficiency (1 mole per mole of 2) a set of silanols, $(Me_3SiO)_n(Me_3Si)_{3-n}SiOH$ ($n = 0–3$)was determined. The molar ratio of the silanols was found to be $2(n = 0)$; $0.1(n = 1)$; $0.7(n = 2)$; $0.2(n = 3)$. So, the major oxidised product in this case was $(Me_3SiO)_2(Me_3Si)SiOH$. It is known that RO- and R_3SiO-substituents at the silicon–silicon bond activate the latter towards electrophilic oxidants [10]. Step-by-step oxidation of three Si–Si bonds in the $(Me_3Si)_3Si$-fragment is predominant and is in agreement with literature data [10]:

Starting sodium tris(trimethylsilyl)silanolate 1 is unreactive toward oxygen; tris(trimethylsilyl)silanol is partially oxidised in a period of several weeks. Consequently, iron(II) atom plays a leading part in oxygen activation and oxidation of Si–Si bonds.

Ate-complex 2 is easily oxidised by 1 equiv. of tetracyanoethylene in DME to form a dark-violet solution, whose EPR spectrum consist of a nine-line signal of the TCNE radical anion. The splitting constant ($a_N = 1.556$ G) agreed with that recorded for the TCNE sodium salt ($a_N = 1.56 \pm 0.002$ G) [11]. The latter forms a dark-violet precipitate when DME is replaced with hexane. The infrared spectrum shows bands at 2200 and 2160 cm^{-1} characteristic of TCNE$^-$ [12]. Filtration of the Na$^+$TCNE$^-$ precipitate followed by removal of the solvent resulted in a rust-brown homoleptic ferric tris(trimethylsilyl) silanolate 4:

$$2 + TCNE \xrightarrow[\substack{2\text{)Hexane}}]{\substack{1\text{)DME}}} \underset{4}{[(Me_3Si)_3SiO]_3Fe} + Na^+TCNE^-$$

3.3. Mössbauer spectra and magnetic measurements

The Mössbauer spectrum for complex 2 at 298 K showed an isomer shift of 0.60(1) mm/s and quadrupole splitting of 0.90(3) mm/s (Fig. 2a and Table 4). These are the first data for a ferrous compound with a FeO$_3$ core. Good correlation of isomer shifts versus coordination number for various $Fe^{2+} O_n$ polyhedra ($n = 8,6$–4)

Fig. 2. Zero-field ^{57}Fe Mössbauer spectra of compounds 2 (a), 3 (b), and products of their thermolysis 2* (c) (400°C) and 3* (d) (200°C).

T= Me₃Si

Table 4
Mössbauer parameters of the compounds 2, 3 and products of their thermolysis (2*) and (3*)

Compound	Site	Area ratio (%)	δ^a (mm/s)	ΔE_Q (mm/s)
2			0.60	0.90
3			1.08	2.12
2*	1	44	0.24	1.12
	2	56	0.20	0.60
3*	1	50	0.24	1.08
	2	50	0.20	0.64

^{a} Relative to Fe metal at room temperature.

was found by F. Menil [13]. The isomer shift for the novel compound 2 (marked with an asterisk) fits well into this correlation (Fig. 3). Interestingly, the isomer shift value for 2 lies in the field between those typical to ferrous high-spin compounds on the one hand and ferrous low-spin compounds on the other hand [14]. The magnetic moment per Fe atom was found to be 4.6 μB in the solid state at room temperature. Thus coordinatively unsaturated trigonal iron (II) is in the high-spin state. The magnetic data for the known complexes of trigonal iron(II) in oxygen environment indicate that the metal centres are also high spin [8,9].

The Mössbauer spectrum for 3 at 298 K is shown in Fig. 2b. The spectrum consist of a quadrupole-split doublet with an isomer shift, δ of 1.08(1) mm/s and a quadrupole splitting, ΔE_Q of 2.12(2) mm/s. These values are in agreement with those for two-valent high spin iron [14]. The observed magnetic moment was found to be 5.6 μB.

3.4. Solid-state thermolysis

Silanolates 2 and 3 are stable thermally up to 100°C for several hours. The complex 2 begins to decompose at 160°C, but 3 at 125°C. The affinity of silicon for oxygen is well known. Since the compounds contain Si–Si bonds the insertion of oxygen into the silicon-silicon bond to form siloxanes under thermolysis should be anticipated. Actually, slow heating of 2 in vacuo (3 deg/min) and subsequent exposure of the sample at 210°C for 1 h leads to tris(trimethyl

Fig. 3. Room-temperature isomer shifts for various Fe^{2+} O_n polyhedra versus coordination number.

silyl)trimethyldisiloxane, $(Me_3Si)_3SiOSiMe_3$, whose yield was 20% per mole of 2. However, tetrakis(trimethylsilyl)silane, $(Me_3Si)_4Si$, also was detected (25%). In the solid residue oligoferrisiloxane was found. The latter is soluble in CH_2Cl_2 or THF. Gel permeation chromatography gave an average molecular weight of 2000 (maximum at 1900 and 3500) and polydispersity of 2.5. The iron content was found to be 11% and the effective magnetic moment 5.2 μB per Fe atom. Treatment of polyferrisiloxane with aqueous HCl under anaerobic conditions gives Fe^{3+} ions which show qualitative reaction with $K_4Fe(CN)_6$ but not with $K_3Fe(CN)_6$. Further heating of 2 up to 400°C results in a slow hydrogen evolution and yields cross-linked, nonsoluble ferrisiloxane (2*). Broad lines in the Mössbauer spectrum of the latter testify that several iron forms with a slightly different environment may be present in the product of thermolysis. It is possible to fit the spectrum to two doublets (Fig. 2c) using an area ratio of 50 : 50 using the parameters in Table 4. The IS and QS values for sites 1 and 2 can be compared with those in the literature for a number of high-spin ferric compounds [14]. Neither α-Fe nor iron oxides were found in the solid products of slow thermolysis. Notice that α-Fe is released in the case of fast thermolysis (> 20°C/min) together with a complicated mixture of organosilicon products.

Thermolysis of 3 up to 200°C gives very similar results to thermolysis of 2. Organosilicon products were $(Me_3Si)_3SiOSiMe_3$ and $(Me_3Si)_4Si$. The solid residue (polyferrisiloxane 3*) is soluble in CH_2Cl_2, THF, consists a broad line doublet in the Mössbauer spectrum (Fig. 2d) that may be fit to two doublets in an area ratio of 44 : 56 using the parameters in Table 4. The effective magnetic moment was found to be (5.9 μB) per Fe atom. Both Mössbauer spectra of products of thermolysis (considering the μB data) are closely related to those typical to polyferrisiloxane containing high-spin octahedral iron(III) [15]. Moreover, at heating we observed some changes in the fitting parameters: the share of site 2 is increased from 50 to 56% owing to diminishing of the site 1 allotment from 50 to 44%. It is known that analogous alteration in quadrupole splitting parameters have been observed at gradual enhancement of the iron content (and, respectively the content of =Fe–O–Fe= fragments in polyferrisiloxane [15]). In the case of thermolysis of iron tris(trimethylsilyl)silanolates we observe the elimination of low molecular weight organosilicon products together with a rise of iron content from 11% (in 3*) to 18% in polyferrisiloxane 2*. Thus, based on the Mössbauer spectra together with the magnetic measurements it should be concluded that two-valent high-spin iron bearing $(Me_3Si)_3SiO$-substituents which are strong σ-donors, does not reduce to metallic iron under slow thermolysis, but turns into a high-spin Fe(III) state.
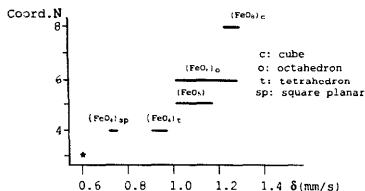
Acknowledgements

References

[1] P.G. Eller, D.C. Bradley, M.B. Hursthouse, D.W. Meek, Coord. Chem. Rev. 24 (1977) 1–95.

[2] D.D. Perrin, W.L.F. Armarego, D.R. Perrin, Purification of Laboratory Chemicals, Pergamon, Oxford, 1980.

[3] A.N. Kornev, T.A. Chesnokova, V.V. Semenov, Yu.A. Kurskii, Russ. Chem. Bull. 44 (1995) 1107.

[4] K.A. Andrianov, V.V. Severnyi, Zh. Obshch. Khim. 32 (1962) 1633.

[5] V.V. Semenov, E.Yu. Ladilina, S.Yu. Khorshev, Yu.A. Kurskii, Zh. Obshch. Khim. 64 (1994) 1652.

[6] V.S. Rusakov, N.I. Chistyakova, Mössbauer Program Complex MSTools, LACAME'92, Buenos Aires, Argentina, July 2, 1992, N7, p. 3

[7] G.M. Sheldrick, Structure Determination Software Program Package (PC version), Siemens Analytical X-ray Instruments, Madison, WI, 1989.

[8] H. Chen, P.P. Power, S.C. Shoner, Inorg. Chem. 30 (1991) 2884.

[9] R.A. Bartlett, J.J. Ellison, P.P. Power, S.C. Shoner, Inorg Chem. 30 (1991) 2888.

[10] B.J. Helmer, R. West, Organometallics 1 (1982) 1463.

[11] W.D. Phillips, J.C. Rowell, S.I. Weissmann, J. Chem. Phys. 33 (1960) 626.

[12] M.F. Rettig, R.M. Wing, Inorg. Chem. 8 (1969) 2685.

[13] F. Menil, J. Phys. Chem. Solids. 46 (1985) 763.

[14] P. Gütlich, R. Link, A. Trautwein, Mössbauer Spectroscopy and Transition Metal Chemistry, Springer, Berlin, 1978.

[15] A.A. Zhdanov, M.M. Levitsky, A.Yu. Dyakonov, O.I. Schego-likhina, A.D. Kolbanowsky, R.A. Stukan, A.G. Knizhnik, A.L. Buchachenko, Izvestiya Acad. Nauk. Ser. Khim. 11 (1990) 2512 (Russ. Chem. Bull.).